

Report ETP - Unstable 2D plume using Fluent

Rafael Graf¹ and Andrea Caldirola¹

¹EPFL

November 4, 2018

Abstract

The aim of this report is to assess if an *unstable thermal boundary layer* affects the *concentration distribution* of an industrial plume. A 2D simulation was performed using the Software *Fluent*, where a stack rejected CO₂ in the atmosphere.

The concentration difference between the stable and unstable thermal boundary layer simulation was practically indistinguishable. Thus, the model simplifications, especially the reduction to a two dimensional model, are discussed for the validity of the simulations as well as the ground boundary conditions.

Introduction

Air pollutants distributions are a big problem all over the world and they are strongly driven by the air temperature gradient. Since the concentration of pollutants at ground level interact directly with people, it is a key factor to monitor.

In this case study, the effect of air temperature lapse rate on a plume of carbon dioxide (one of the most common pollutants) coming out from a stack is evaluated.

The temperature of air is characterized by a vertical temperature gradient, this is affecting the atmospheric air stability and thus the pollutant distribution through the APBL (Atmospheric Planetary Boundary Layer).

For a neutral APBL, the mixing is mainly driven by the turbulences of the Inertial Sub-Layer (ISL) wind, whose height spans between 10-20% of the APBL. Here the vertical wind speed profile can be described by log-velocity profile ([Jirka, 2005](#)) :

$$U(z) = \frac{U_*}{k} \ln \left(\frac{z}{z_0} \right) \quad (1)$$

Where U_* = shear velocity; $\kappa=0,42$ is the Von Karman constant; z_0 =roughness height.

The idealized neutral conditions described above are rarely strictly valid. Indeed, heating and cooling within the boundary layer result in temperature differences, which equate to density differences. Thus, buoyancy effects and stability/instability are important processes in the APBL.

It is possible to state the Equilibrium conditions of the APBL, with reference to the Adiabatic Lapse Rate (ALR) Γ . This gradient (eq. 4) is computed by combining the first law of thermodynamic (eq. 2) and the barometric equation (eq. 3) :

$$dq = dh - vdp = C_p dT - \frac{1}{p} dP = 0 \quad (2)$$

$$\frac{dP}{dZ} = -pg \quad (3)$$

$$\Gamma = \frac{dT}{dZ} = -\frac{g}{C_p} = 9.8 \frac{K}{km} \quad (4)$$

Where for dry air $C_p = 1005 \text{ [J/K]}$.

The idea is to consider those two different stability cases:

- Unstable: $-\frac{dT}{dZ} > \Gamma$
- Strongly stable: $-\frac{dT}{dZ} < \Gamma$

In the first case, the absolute value of the temperature gradient is higher than the ALR. This case is unstable and occurs during the day, solar radiation heats the bottom air, so warm air at the bottom rises, creating enhanced vertical velocities. That is, regions of warm upward-moving air, called thermals, are surrounded by layers of cold downward moving air. In this case, the plume generated by a point source will be characterized by the so-called looping.

In the second case, the absolute value of the temperature gradient is much lower than the ALR. This case is stable, like in the night, when the bottom layer cools down rapidly, and the boundary layer develops in a stable density profile (heavy air below lighter air). In this case, the plume generated by a point source will be characterized by the so-called fanning.

The concentration downstream a release of a continuous point source has already been covered by literature (Csanady, 1973):

$$C(x, y, z) = \frac{M}{2\pi u \sigma_y \sigma_z} \left[\exp\left(-\frac{y^2}{2\sigma_y^2} - \frac{(z-h)^2}{2\sigma_z^2}\right) + \exp\left(-\frac{y^2}{2\sigma_y^2} - \frac{(z+h)^2}{2\sigma_z^2}\right) \right] \quad (5)$$

with M the mass flow, u the velocity, the slack height h and the two variances σ_y and σ_z , which can be approximated in the near field by the turbulent intensities times the horizontal distance $i_y x$ and $i_z x$ respectively (Jirka, 2005). However, as we are simulating in two dimensions, equation 5, must be fitted as there is no diffusion in σ_y . So the problem simplifies to an advective one point source release, with a mirror condition (eq. 6):

$$C(x, z) = \frac{\dot{m}}{\sqrt{2\pi}\bar{u}\sigma_z} \left[\exp\left(-\frac{(z-h)^2}{2\sigma_z^2}\right) + \exp\left(-\frac{(z+h)^2}{2\sigma_z^2}\right) \right] \quad (6)$$

With the variance $\sigma_z = i_z \cdot x$, increasing linearly with the distance to the stack.

Method

The simulation was performed using the Software *Fluent*. The energy equations and the species transport were enabled, and the k-epsilon standard model was used. The 2D simulation was performed on a section with dimensions of 300 x 60 meters. The stack of dimension 1 x 10 m was placed at 30 m of the wind inlet (left side). A global mesh side of 1 m was used with a refinement of 0.2 m around the plume. A total number of 19918 cells were used. The final mesh can be seen in Figure 1.

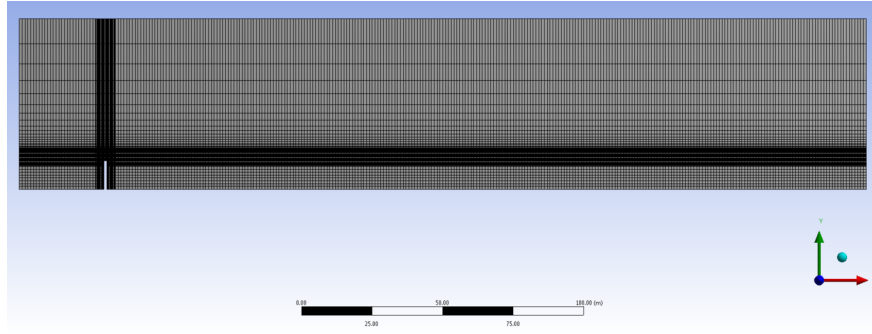


Figure 1: Mesh of the simulations

Following boundary conditions were applied on the different surfaces:

- Upper boundary: Pressure outlet
- Right boundary: Pressure outlet
- Under boundary (ground): Wall with no slip condition, at temperature T_g
- Left boundary (wind inlet): Velocity profile $U_{in}(y)$, at temperature $T_{in}(y)$
- Wall of the chimney: Wall with no slip condition, adiabatic
- Chimney outlet: CO_2 at 453 K, with a velocity of 0.5 m/s

And for two different simulation cases:

Simulation 1: Stable thermal boundary condition.

$$T_g = 288 \text{ K}, \quad T_{in} = T_g + \frac{5}{30} \cdot y$$

where y is the vertical height in meter starting from the ground.

Simulation 2: Unstable thermal boundary condition.

$$T_g = 293K, \quad T_{in} = T_g - \frac{5}{30} \cdot y$$

And the velocity profile in both simulation can be calculated as presented in the introduction:

$$U_{in}(y) = \frac{U_*}{\kappa} \ln\left(\frac{y}{y_0}\right)$$

starting from $y_0 = 1$ (roughness height for large towns and cities), and with $U_* = 0.52$, (velocity of 3 m/s at 10 m)

Both simulations were run by using a first order model and iterating until all residual went below $10e-3$.

Results

The main results, consisting of temperature, mass fraction and velocity profile (fig. 2, 3 and 4) are depicted here. The figures of the first case are representative of both simulations as the solutions of the two cases are quasi identical (fig. 5).

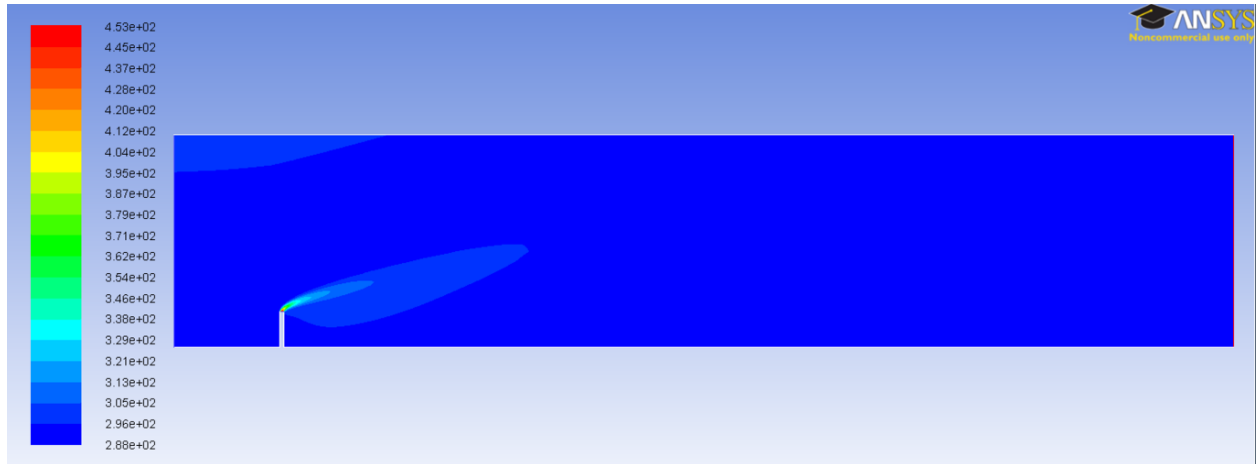


Figure 2: *Case 1*. Temperature [K] distribution.

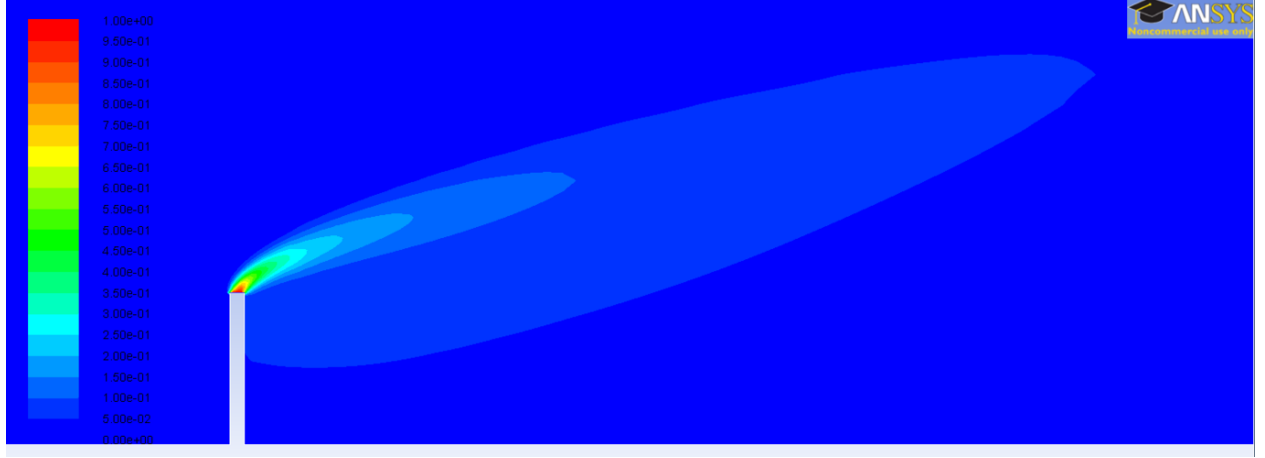


Figure 3: *Case 1*. CO2 mass fraction [-] distribution.

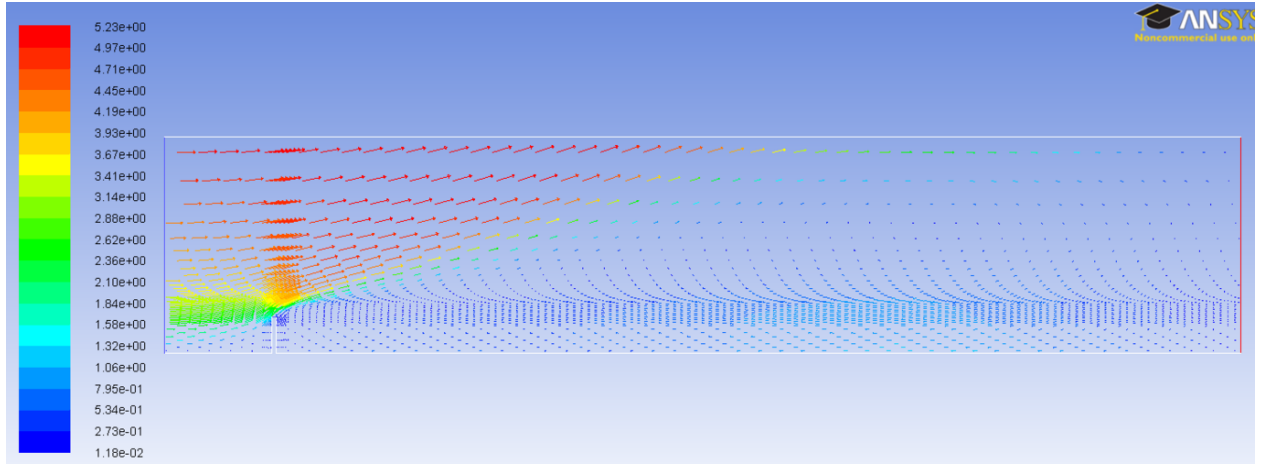


Figure 4: *Case 2*. Wind speed vectors (modulus [m/s]).

Analysis and Discussion

The obtained results are not the expected ones. Indeed a higher difference was expected between the two cases. A higher variance and a bigger fluctuation of the maximal position was awaited especially in case two, where unstable thermal condition were used.

In order to have some more quantitative values, the results were analysed with the post-processing software of Fluent *CFD-Post*. The CO2 mass fraction was evaluated on two vertical sections, placed at 1 and 10 m on the leeward side of the stack. That allowed to compare the mass fraction profile of the two simulation with the one computed by using the 2D advection-diffusion equation (eq. 6, fig. 5) and to determine the values showed in figure 6.

The CO2 mass fraction profiles (dashed lines in figure 5) computed by using the 2D advection-diffusion equation, represent the same, but simplified case, where no convection and plume rise is considered. The equation (6) used for computing the reference profile was parametrized with a turbulence intensity index (i_z) of 0.3, and a mass flow of 3.6 kg/s to best fit with the simulations.

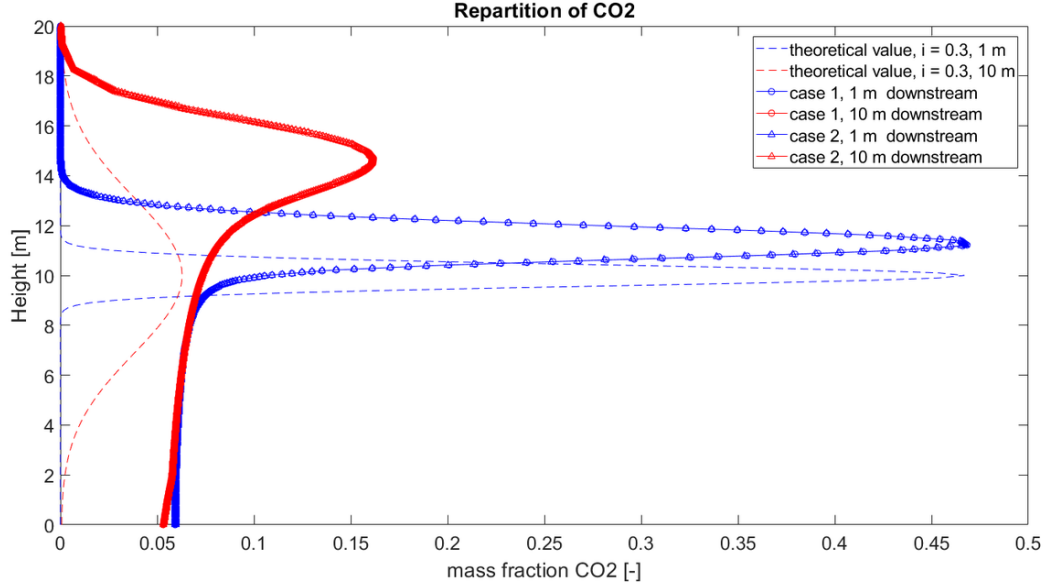


Figure 5: Theoretical and simulated CO2 repartition

	First case		Second case	
Distance to stack downstream:	1 m	10 m	1 m	10 m
CO2 max mass fraction [-]	0.468	0.162	0.468	0.162
Max CO2 position y [m]	11.2	14.7	11.2	14.7
Variance [-]	0.0102	0.0015	0.0103	0.0015
CO2 ground mass fraction [-]	0.059	0.053	0.059	0.053

Figure 6: Table presenting the position and variance of the two simulations

The highest difference between the theoretical and simulated values (neglecting the plume rising) can be observed *under the plume*. Indeed, the CO2 concentration levels are way larger in the simulations. However, it can be explained observing the detail of the wind vectors (fig. 7). The flow is blocked by the chimney, which considerably reduces the magnitude of the wind force, and also creates a large recirculating zone where the CO2 gets trapped in. These observations are not representative of the reality, since the flow will circumvent the stack, keeping the wind profile nearly unchanged.

Several methods could be employed to improve the simulations. To improve the models accuracy, only the stack outlet could be modelled or the simulation could be made in 3 dimensions, allowing the wind to circumvent the stack.

To increase the effect of the instability, modelling the radiation of the sun on the ground could be an option. Indeed, according to Pasquill's (1962) stability categories (from (Csanady, 1973)), a strong radiation - compared to no radiation - increases the instability of the flow. Therefore, changing the boundary condition of the ground from constant temperature to a heat flux should increase the buoyancy effects.

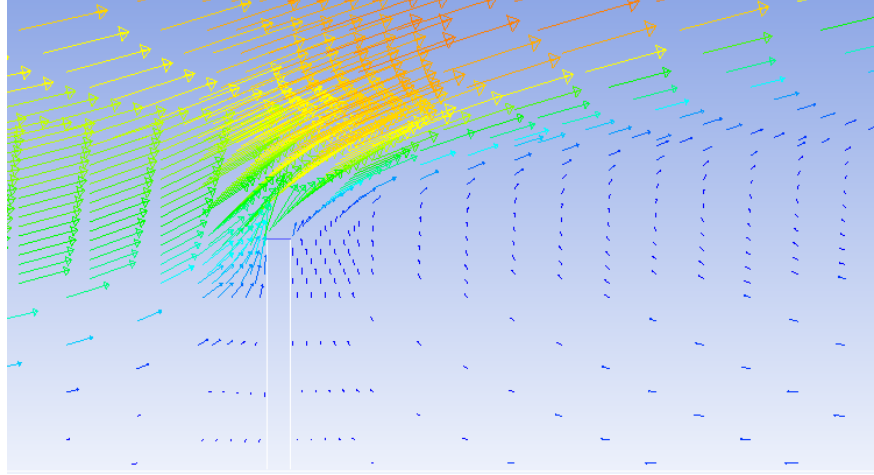


Figure 7: *Case 1*. Detail of the wind speed vectors around the stack.

Conclusion

Out of these simulations, two main conclusions can be drawn. First, a two dimensional model does not reflect the physical phenomenons with complete accuracy when the solid stock is modelled. The stock completely blocks the wind flow and also creates a recirculation zone. However, only modelling the stock outlet or adding a third dimension should increase the simulations validity.

Second, no concentration difference could be observed between the stable and unstable boundary condition. But including the solar irradiation in the unstable case, could increase the instabilities of the flow.

References

- G. T. Csanady. *Turbulent Diffusion in the Environment*. Springer Netherlands, 1973. doi: 10.1007/978-94-010-2527-0. URL <https://doi.org/10.1007%2F978-94-010-2527-0>.
- Scott A. Socolofsky & Gerhard H. Jirka. *Special Topics in Mixing and Transport Processes in the Environment*. Coastal and Ocean Engineering Division, 2005.